Article

Ethylene Polymerization by 2-Methyl-8-(benzimidazol)quinolyliron(II) Pre-Catalyst: a DFT Understanding its Chain Propagation and Transfer

Wenhong Yang,[a] Toshiaki Taniike,[b] Minoru Terano,[b] Yan Chen[a] and Wen-Hua Sun*,[a]

[a]Key Laboratory of Engineering Plastics and Beijing National Laboratory for Molecular Science, Institute of Chemistry, Chinese Academy of Sciences, 100190 Beijing, China

[b]School of Materials Science, Japan Advanced Institute of Science and Technology, 1-1 Asahidai, Nomi, 923-1292 Ishikawa, Japan

O mecanismo de polimerização do etileno com o pré-catalisador 2-metil-8-(benzimidazol) quinoliliron(II) foi investigado através da teoria de densidade funcional (DFT), ilustrando possíveis intermediários com configurações geométricas e de spin. De acordo com o grupo ligado ao núcleo ferro, metila ou etila, as barreiras de energia para a inserção de etileno foram extensivamente calculadas. Dentro das espécies ferro-metila, ambos os estados, transição e fundamental, favorecem as configurações com estado de alto spin (quinteto); enquanto as espécies ferro-etila preferem o estado de baixo spin. De acordo com as barreiras de energia, a propagação de cadeia é mais favorável que a transferência de cadeia para pré-catalisador bidentado de ferro, que é bem consistente com as observações experimentais.

The ethylene polymerization mechanism of the 2-methyl-8-(benzimidazol) quinolyliron(II) pre-catalyst is investigated by the DFT calculations, illustrating the possible intermediates with their geometrical and spin configurations. Regarding either methyl or ethyl group bonding on iron cores, the energy barriers for ethylene insertion have been extensively calculated. Within the iron-methyl species, both resting state and transition state favor the configurations at high-spin state (quintet); whilst the iron-ethyl species prefer the low-spin state. According to the energy barriers, the chain propagation is more favorable than chain transfer for the bidentate iron pre-catalyst, which is well consistent with the experimental observation.

Keywords: density functional theory, iron complex pre-catalyst, ethylene polymerization, chain propagation, chain transfer

Introduction

Late-transition metal complex pre-catalysts have attracted many attentions in ethylene polymerization[1,2] since the innovative observations by Brookhart and co-workers.[3-5] One of the advantages is the well-defined complexes that provided the single-site active species and resulted in the finely controllable polymeric materials, and many achievements have been made in the past decades.[6-9] Concerning the economic and environmental issue, the iron-based pre-catalysts are of great interest, moreover their products like highly linear oligomers and polyethylenes are industriously demanding. Therefore more efforts have been devoted to modify bis(imino)pyridine iron comlexes[10,11] as well as developing alternative iron complex pre-catalysts through designing new ligand compounds.[12-16]

Various thermodynamic processes have been considered on the base of the reaction pathways with different activation energies of active species. Regarding the coordination polymerization process, molecular modeling could elucidate the states and structures of active centers, as well as catalytic mechanisms. Besides some experimental approaches to the intermediates and the polymerization mechanism of the iron complex pre-catalysts,[17-20] it has been developing to explore computational study on the complex pre-catalysts by the density functional theory (DFT) method[21] on the basis of fast development of theory methods and computer capability; the theoretical calculations provide the useful tools to explore the reaction mechanism[22-28] as well as the catalytic activities.[29]

Herein referring the experimental observations by the 2-methyl-8-(benzimidazol) quinolyliron(II) chloride pre-catalysts (Scheme 1),[30] the DFT calculations have been conducted to explore the catalytic mechanism. The insertion reactions for the propagation process of ethylene into the models, either Fe-methyl or Fe-ethyl, have been focused along with their chain transfer processes. Relied on the active species and transition states of individual reaction steps, all the possible intermediates either at high-spin or low-spin states have been considered. The calculation results illustrated the pathway for favorable chain propagation over chain transfer, being consistent to the experimental observations producing polyethylenes instead of oligomers.
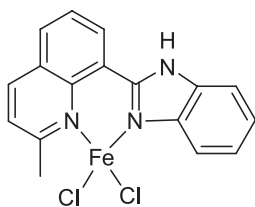
Scheme 1. Structural model of iron complex pre-catalyst.

Experimental

Using the DMOL3 program, the DFT calculations were performed.[31] The electronic structures of the molecular systems were described by double-numerical basis sets with polarization functions (DNP)[31] combination with effective core potentials.[32,33] Two types of functions BP and B3LYP were employed to optimize the molecular structures in determining the calculation parameters.[34,35] Transition states were optimized along an imaginary frequency corresponding to the reaction coordination. The criteria for transition state optimization were 2×10^{-5} Hartree in energy and 4×10^{-3} Hartree/Å in force. For SCF calculations the convergence criteria were 1.0×10^{-5} Hartree, whilst the geometry optimization and energy the criteria were 2.0×10^{-5} Hartree and 4×10^{-3} Hartree/Bohr for the maximum force, respectively.

Regarding spin states of iron atom, there are three of singlet, triplet and quintet. In the literature of bis(imino) pyridyliron pre-catalysts, the singlet electronic state of Fe (II) was the most favorable for the propagation and termination reaction;[36] however, it was also reported the high (quintet or triplet) spin state in the electronic configuration of Fe (II) within the propagation reaction.[37-39] The energy difference between high-spin state and low-spin state was relatively small, therefore three spin states were subsequently considered for all the structures in chain propagation and chain transfer reactions. Regarding Fe^{+}-R

as the active species, the R group as both methyl and ethyl were taken into account. According to the Brookhart-Green mechanism,[40] the agostic interaction between hydrogen atoms in alkyl chain and central metal plays an important role during the ethylene polymerization for bridged type transition metal catalyst. The α-agostic and β-agostic modes were investigated for the more realistic model by ethyl group. The orientations of the ethyl group connected with the center Fe atom in different orientations were also considered for the C1-symmetric catalyst. In the following, the coordination energy (ΔE_C) is defined as the difference of the electronic energies between π-complex coordinated with ethylene molecule and the resting state. The transition state energy (ΔE_T) stands for the difference of the electronic energies between transition state and resting state.

Results and Discussion

Optimized structure for 2-methyl-8-(benzimidazol) quinolyliron dichloride

Prior to discuss the propagation process of the ethylene molecule, the geometrical structures of the model pre-catalyst were optimized in the comparison with experimental results. Their calculated structural parameters at different spin states and various exchange-correlation functions were tabulated in Table 1.

To simplify the model molecule of experimental 2-methyl-8-(benzimidazol-2-methyl) quinolyliron dichloride,[30] but being relied on the experimental observation of crystal data, the methyl group linked on benzimidazole was omitted in the calculation; the selected bond lengths and bond angles related to the central iron atom were shown in Table 1, illustrating calculated configurations at various parameters. In the structural view, the standard deviation values δ between calculated results and experimental crystal data were obtained with different functions for either high-spin state or low-spin state. In general, the lowest energy was approved for the high-spin state by both BP and B3LYP functions, individually. Comparably the calculation geometry with BP function at quintet showed better coincidence than others. Since the δ values among various spin states were close, all of these three spin states were explored in investigating the polymerization reaction for the model catalyst with BP function.

Methyl group model for propagation process

With the illustrated structure of model complex, two chloride anions were imaginably exchanged by methyl

Table 1. Comparisons of the structures between experimental observations and calculated results at various spin states coupled with BP and B3LYP function, in which δ was the standard deviation values

			Bond length / Å			
	Ex.	bp-S	bp-T	bp-Q	b3lyp-S	b3lyp-T	B3lyp-Q
Fe-N1	2.027	1.893	1.888	2.083	1.915	1.922	2.118
Fe-N2	2.143	1.928	2.013	2.229	1.964	2.113	2.279
Fe-Cl1	2.255	2.220	2.223	2.219	2.258	2.257	2.234
Fe-Cl2	2.270	2.238	2.232	2.233	2.263	2.265	2.251
N1-C10	1.327	1.335	1.343	1.333	1.312	1.319	1.318
N3-C10	1.371	1.384	1.382	1.376	1.368	1.364	1.366
δ	–	4.4	3.41	2.28	3.5	1.96	3.22

			Bond angle / degree			
	Ex.	bp-S	bp-T	bp-Q	b3lyp-S	b3lyp-T	b3lyp-Q
N1-Fe-N2	89.2	95.4	93.8	85.8	96.2	93.1	86.8
N1-Fe-Cl1	112.9	103.3	108.7	112.5	100.8	105.6	115.8
N1-Fe-Cl2	110.1	97.1	104.9	107.3	98.2	104.9	103.3
N2-Fe-Cl1	109.8	100.6	112.3	98.3	106	105.9	97.3
N2-Fe-Cl2	117.4	106.3	121.4	119.5	97.8	117.2	113.4
Cl1-Fe-Cl2	114.9	144.4	112.9	126.5	147.5	124.5	131.2
δ	–	14.6	4.06	6.80	16.6	5.74	8.79
ΔE	–	3.39	8.89	0	7.44	8.12	0

group to create the cationic active species; which were proposed according to general images with the co-catalyst MAO acting the methylation.[41-43] The methylated cationic species were the resting states, and further process the insertion step for the chain propagation through the introduction of ethylene molecule. With the process of chain propagation, the geometries at each states were illustrated in Figure 1, including the resting state for methyl cationic species (Figure 1a), π-coordinated intermediate with ethylene molecule (Figure 1b), transition state (Figure 1c) and the product (Figure 1d) at triplet state as an example.

Concerning the reaction mechanism, the variations of selected bond lengths were indicated for the insertion process in Figure 1. There were around 1.901 Å for Fe-N bond and 1.935 Å for Fe-C bond in the resting state; these values were slightly enlarged to 1.923 Å and 1.958 Å, respectively, in the π-coordinated intermediate due to electronic donation by the ethylene molecule with its carbon and Fe distance as 2.159 Å in the line of π interaction.[19] In the transition state (Figure 1c), the bond lengths of Fe-N and Fe-C were further enlarged to 1.993 Å and 2.033 Å, respectively, meanwhile the bond length for ethylene (C=C) was also extended from 1.343 Å to 1.456 Å, forming a four-membered ring. With the chain propagation happened (Figure 1d), the obtained species had a propyl chain, and
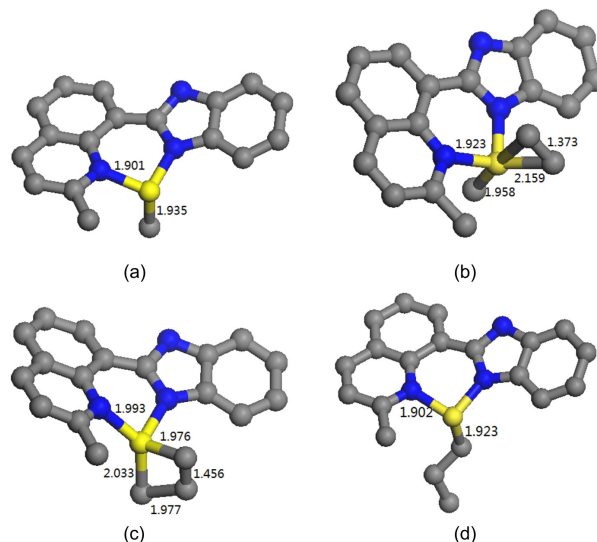
Figure 1. The structure of the resting state for methyl cationic species (a); π-coordinated intermediate (b); transition state (c) and the product (d), respectively. For the sake of clarity, hydrogen atoms were omitted.

similar to its resting state with the lengths of Fe-N and Fe-C bonds. The chain propagation process is agreed with the classical Brookhart-Green mechanism.[40]

The energy variations at different spin states were collected in Table 2, based on different structural geometries. The relative data of energy were obtained at resting states. The ΔE_C indicated the energy difference of

the π-coordinated intermediate to the resting state, and the ΔE_T showed the energy difference from transition state to the resting state.

Table 2. The values for the coordination energy ΔE_C and the transition energy ΔE_T for each reaction path in methyl group

	Q	T	S
Relative energy / (kcal mol⁻¹)	0	5.59	4.39
ΔE_C / (kcal mol⁻¹)	−6.84	−7.41	−7.82
ΔE_T / (kcal mol⁻¹)	5.17	8.99	9.46

All the energy values were obtained comparing the optimized energy with the resting state at quintet which indicated the lowest energy value. Accordingly, the energy profiles were plotted in Figure 2, showing the energy variations with the ethylene insertion at the spin state potential energy surface (PES).
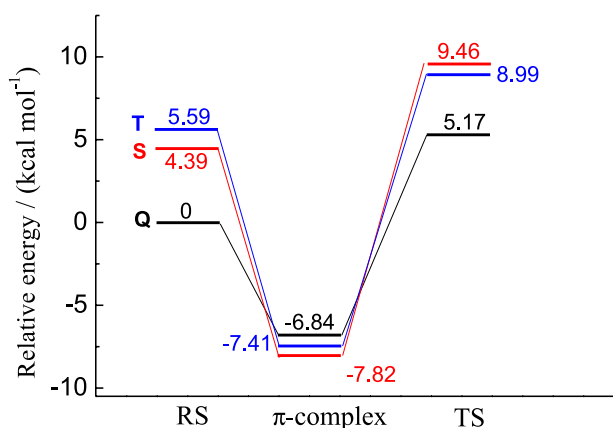
Figure 2. The energy profiles for propagation process at each spin state with methyl model, including resting state (RS), π-complex and transition state (TS).

The resting state at quintet was the most stable configuration with the energy of 5 kcal mol⁻¹ lower than that of triplet and singlet spin state; the coordination energy ΔE_C was −6.84 kcal mol⁻¹ and the ΔE_T was 5.17 kcal mol⁻¹, indicating the insertion energy barrier about 12.01 kcal mol⁻¹. In comparison, the insertion energies were 17.28 kcal mol⁻¹ for singlet spin state and 16.40 kcal mol⁻¹ for triplet spin state, respectively.

Therefore, the reactions were favorably carried out with the quintet PES.

The system for sequential chain propagation

Regarding the sequential propagation process, the plausible system involves the presence of the β-agostic interaction between alkyl hydrogen and metal center, in which the ethyl group represents the existing alkyl chain. Similar to the above model images, the resting states containing ethyl group were optimized at all spin states as well as with the different orientations of alky chain in the α-agostic and β-agostic modes. The ethylene insertion was investigated and the obtained energy values were listed in Table 3.

Regarding α-agostic mode, the high-spin configuration was more stable than the low-spin configuration; the energy values increased in the order as quintet < triplet < singlet, and the energy difference between singlet and quintet can be reached up to 23.4 kcal mol⁻¹. Within β-agostic mode, the low-spin configuration had a lower energy value and was more stable than that configuration at high-spin state; its most stable structure was optimized at triplet and confirmed within all the resting states. Checking the β-agostic mode at quintet state, the distance between the β-hydrogen and iron atom was around 2.7 Å (out of the normal agostic interaction), which was larger than that within its singlet and triplet (ca. 1.7 Å). The β-agostic interaction was more favorable to the low spin states, therefore there was hardly β-agostic interaction existing in this iron model at high-spin state; which is consistent to the literature.[44] In comparison with above results of the resting state in methyl group preferring high-spin states, the resting state with ethyl group showed the low-spin state (triplet) to its β-agostic mode. The optimized geometries for α-agostic and β-agostic modes with various chain orientations and spin configurations were showed in Figure 3.

Subsequently, the resting state configurations of the β-agostic mode at triplet were further investigated to illustrate the chain propagation process (Figure 4), according to the similar interpretation used for the above model of methyl group. Compared to resting state with the bond lengths of Fe-N and Fe-C 2.076 Å to 2.011 Å,

Table 3. The results for the coordination energy ΔE_C and the transition energy ΔE_T for each reaction path in ethyl group

	α-agostic1			α-agostic2			β-agostic		
	Q	T	S	Q	T	S	Q	T	S
Relative energy / (kcal mol⁻¹)	3.14	9.1	23	3.01	5.8	23.4	5.36	0	3.7
ΔE_C / (kcal mol⁻¹)	−3.41	−4.24	−1.59	−2.79	−3.13	−3.22	−6.39	−4.29	−12.30
ΔE_T / (kcal mol⁻¹)	8.15	6.73	13.01	8.71	7.57	6.07	9.50	8.04	4.68
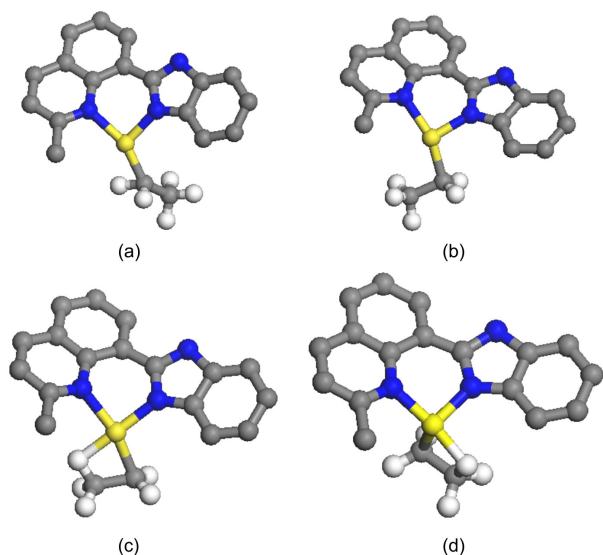
Figure 3. The resting state configurations for α-agostic mode at high-spin state with the alkyl chain in the right direction (a) and left direction (b) and β-agostic mode at triplet (c) and singlet states (d), respectively. For the sake of clarity, hydrogen atoms were omitted except for ethyl chain.

the π-coordinated intermediates showed stronger bonding with Fe-N 1.957 Å and Fe-C 1.997 Å, respectively, along with the distance between ethylene carbon and iron center as 2.090 Å, which was slightly shorter than that in methyl group. In the transition state, the bond length of Fe-N bond and Fe-C bond enlarged to 2.175 Å and 2.004 Å to assist the forming of the four-membered ring in the consistence of the presence of β-agostic interaction. In addition, the C=C bond of ethylene was also extended into 1.443 Å.
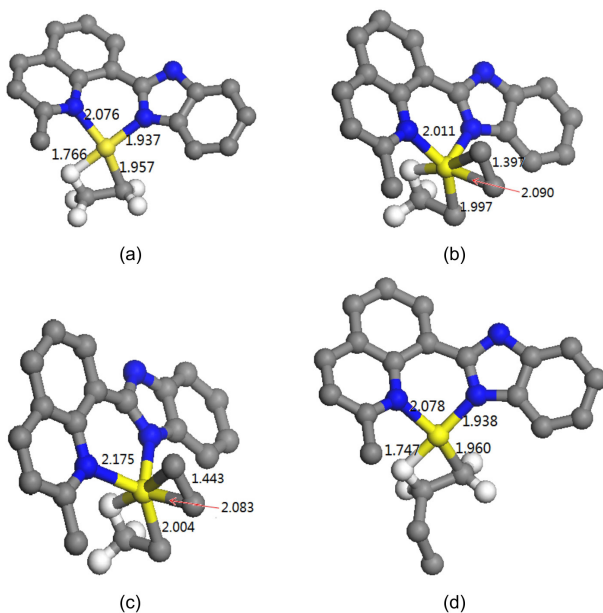
Figure 4. The structure for the resting state configuration of β-agostic mode at high-spin state (a); π-complex (b); transition state (c) and the product (d), respectively. For the sake of clarity, hydrogen atoms were omitted except for β-hydrogen.

After ethylene insertion to achieve another propagation, the new resting state showed the similar bond lengths of their Fe-N and Fe-C bonds as well as the Fe-H (β-agostic) bond.

According to Table 3, with the coordination energy ΔE_C and the transition energy ΔE_T values, the quintet state showed similar energy values for the α-agostic1 and α-agostic2 modes. Regarding its β-agostic mode, the energy values for resting state and π-coordinated intermediate were 5.36 and −6.39 kcal mol^{-1}, respectively; however, the β-agostic interaction at quintet state was very unstable with longer length between β-H and iron, which could be interpreted as an actual α-agostic mode with high energy. The calculated reaction barrier at quintet was 10.94 kcal mol^{-1}. In contrast, at triplet, the coordination energy varied from −3.13 to −4.29 kcal mol^{-1} and the transition state energy varied from 6.73 to 8.04 kcal mol^{-1}, meanwhile its insertion energy was 9.86 kcal mol^{-1}, which was slightly lower than that at quintet. At singlet, the configuration for resting state with β-agostic mode was very stable in the comparison with its α-agostic mode; the energy difference reached up to 20 kcal mol^{-1}, indicating a high energy barrier from β-agostic mode into α-agostic mode. The coordination energy was the lowest one with the value −12.30 kcal mol^{-1} and the lowest transition energy 4.68 kcal mol^{-1}, leading to the insertion energy as 17 kcal mol^{-1}; this was the highest reaction energy among this three spin states. Therefore, the chain propagation takes place more easily at high-spin state. The correspondent structures of transition states were illustrated in Figure 5 regarding the α-agostic mode at quintet and triplet states as well as β-agostic mode at triplet and singlet.

Chain transfer process

On the basis of the β-agostic hydrogen interaction with central iron, the chain transfer process was investigated with the transition state structure demonstrated in Figure 6a and 6b, illustrating a nice model of the chain termination happened with the transformation of a β-agostic hydrogen from the β-carbon onto an approaching ethylene molecule.

At quintet, all trials for the transition state with the β-H transfer were unsuccessful due to its highly unstable state. Therefore, the energy variations were obtained at triplet and singlet state for π-coordinated intermediates and transition states to explore the plausible pathways, and the calculated results were listed in Table 4. All the energy values were compared with the lowest energy value of resting state with β-agostic mode at triplet.

The coordination energies ΔE_C are −13.4 kcal mol^{-1} at triplet and −14.69 kcal mol^{-1} at singlet state, respectively; these values were higher than the energy values with chain

(a) α-1-Q   (b) α-1-T   (c) α-2-Q

(d) α-2-T   (e) β-T   (f) β-S
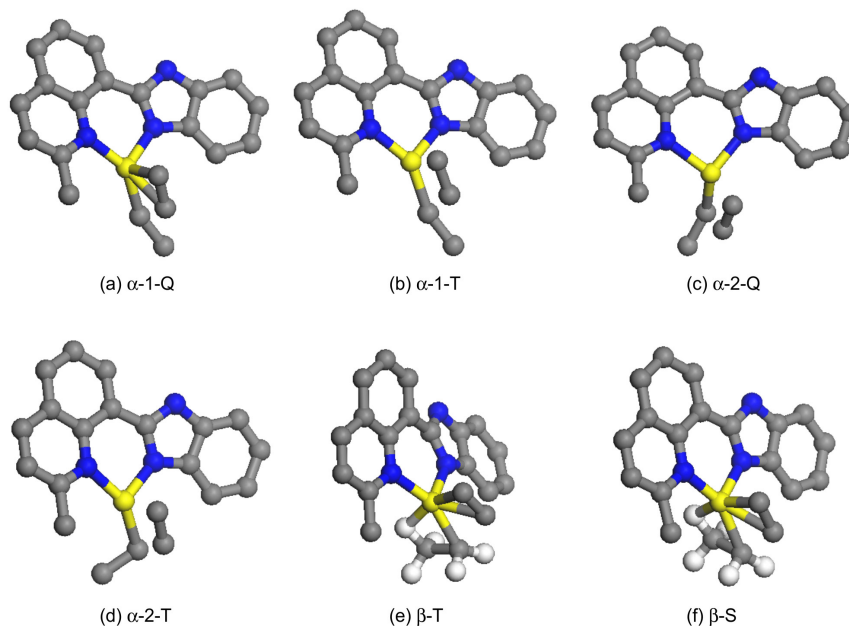
Figure 5. The transition state structures of chain propagation process in ethyl group for the different reaction path.

(a)   (b)
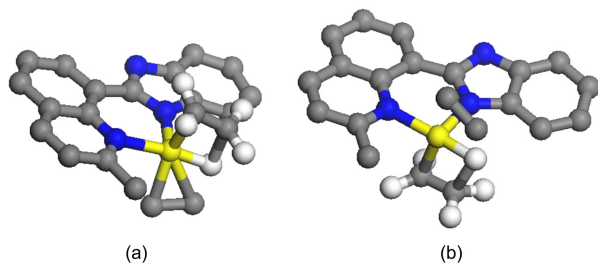
Figure 6. The transition state structures for chain transfer process at triplet state (a) and singlet state (b).

Table 4. The coordination energy ΔE_C for π-complex and the transition energy ΔE_T for transition state at each spin state for β-H transfer reaction

	β-HT		
	Q	T	S
Relative energy / (kcal mol^{-1})	5.54	2.16	3.22
ΔE_C / (kcal mol^{-1})	–	−13.40	−14.69
ΔE_T / (kcal mol^{-1})	–	4.70	6.11

propagation in both modes with either methyl or ethyl group. The transition energy ΔE_T for the chain transfer reaction at these spin states were 4.70 and 6.11 kcal mol^{-1}, individually, meanwhile the corresponding insertion energy barriers were 18.10 and 20.80 kcal mol^{-1}. In comparison with the energy barriers for chain propagations, the β-H transfer reactions required much higher energies; therefore, the catalytic system preferred to have chain propagation instead of chain transfer reaction. The calculated results agreed to achieve polymers, which were approved by the experimental observations with obtaining polyethylenes with high molecular weights.[30]

Conclusions

The ethylene polymerization by 2-methyl-8-(benzimidazol)quinolyliron(II) dichloride was extensively investigated by the density functional theory calculation for both models with methyl and ethyl group. The various spin states were investigated to optimize their reasonable geometrical structures with consistent to the experimental crystal observations. Based on the model with methyl group as the initial stage, the configuration for resting state at quintet was the most stable one; the reaction barrier at quintet was the lowest in the comparison with its triplet and singlet analogs about 12.01 kcal mol^{-1}. In the subsequent propagation process, happened to the model with ethyl group regarding the α-agostic and β-agostic modes, the most stable resting state was the configuration with β-agostic mode at triplet; the correspondent reaction barrier at quintet and triplet were close with the value to be 10.94 and 9.86 kcal mol^{-1}, respectively, which was much lower than that of singlet. In competition of chain transfer and propagation, the energy barrier was higher within chain transfer than chain propagation, therefore the current model complex pre-catalysts provided polyethylenes with higher molecular weights, consistent to the experimental observations.[30] In a word, the simulation methodology could be helpful in designing complex pre-catalysts in ethylene polymerization.

Acknowledgments

References

1. Zhang, W.; Sun, W.-H.; Redshaw, C.; *Dalton Trans.* **2013**, *42*, 8988.

2. Sun, W.-H.; *Adv. Polym. Sci.* **2013**, 258, 163.

3. Johnson, L. K.; Killian, C. M.; Brookhart, M.; *J. Am. Chem. Soc.* **1995**, *117*, 6414.

4. Killian, C. M.; Tempel, D. J.; Johnson, L. K.; Brookhart, M.; *J. Am. Chem. Soc.* **1996**, *118*, 11664.

5. Small, B. L.; Brookhart, M.; Bennett, A. M.; *J. Am. Chem. Soc.* **1998**, *120*, 4049.

6. Wang, C.; Friedrich, S.; Younkin, T. R.; Li, R. T.; Grubbs, R. H.; Bansleben, D. A.; Day, M. W.; *Organometallics* **1998**, *17*, 3149.

7. Speiser, F.; Braunstein, P.; Saussine, L.; *Organometallics* **2004**, *23*, 2625.

8. Gibson, V. C.; Redshaw, C.; Solan, G. A.; *Chem. Rev.* **2007**, *107*, 1745.

9. Wang, S.; Sun, W.-H.; Redshaw, C.; *J. Organomet. Chem.* **2014**, *751*, 717.

10. Britovsek, G. J. P.; Bruce, M.; Gibson, V. C.; Kimberley, B. S.; Maddox, P. J.; Mastroianni, S.; McTavish, S. J.; Redshaw, C.; Solan, G. A.; *J. Am. Chem. Soc.* **1999**, *121*, 8728.

11. Chen, Y.; Qian, C.; Sun, J.; *Organometallics* **2003**, *22*, 1231.

12. Paulino, I. S.; Schuchardt, U.; *J. Mol. Catal. A: Chem.* **2004**, *211*, 55.

13. Cowdell, R.; Davies, C. J.; Hilton, S. J.; Marechal, J.-D.; Solan, G. A.; Thomas, O.; Fawcett, J.; *Dalton Trans.* **2004**, 3231.

14. Karam, A.; Tenia, R.; Martinez, M.; Lopez-Linares, F.; Albano, C.; Diaz-Barrios, A.; Sanchez, Y.; Catari, E.; Casas, E.; Pekerar, S.; Albornoz, A.; *J. Mol. Catal. A: Chem.* **2007**, *265*, 127.

15. Small, B. L.; Rios, R.; Fernandez, E. R.; Carney, M. J.; *Organometallics* **2007**, *26*, 1744.

16. Appukuttan, V. K.; Liu, Y.; Son, B. C.; Ha, C.-S.; Suh, H.; Kim, I.; *Organometallics* **2011**, *30*, 2285.

17. Gibson, V. C.; Humphries, M. J.; Tellmann, K. P.; Wass, D. F.; White, A. J. P.; Williams, D. J.; *Chem. Commun.* **2001**, 2252.

18. Bryliakov, K. P.; Semikolenova, N. V.; Zakharov, V. A.; Talsi, E. P.; *Organometallics* **2004**, *23*, 5375.

19. Bart, S. C.; Chlopek, K.; Bill, E.; Bouwkamp, M. W.; Lobkovsky, E.; Neese, F.; Wieghardt, K.; Chirik, P. J.; *J. Am. Chem. Soc.* **2006**, *128*, 13901.

20. Bowman, A. C.; Milsmann, C.; Atienza, C. C. H.; Lobkovsky, E.; Wieghardt, K.; Chirik, P. J.; *J. Am. Chem. Soc.* **2010**, *132*, 1676.

21. Ziegler, T.; *Chem. Rev.* **1991**, *91*, 651.

22. Cavallo, L.; Guerra, G.; Corradini, P.; *J. Am. Chem. Soc.* **1998**, *120*, 2428.

23. Niu, S.; Hall, M. B.; *Chem. Rev.* **2000**, *100*, 353.

24. Klaus, A.; Gerhard, F.; Vidar, R. J.; Ralph, K.; *Chem. Rev.* **2000**, *100*, 1457.

25. Flisak, Z.; *Macromolecules* **2008**, *41*, 6920.

26. Liu, Z.; Zhong, L.; Yang, Y.; Cheng, R. H.; Liu, B. P.; *J. Phys. Chem. A* **2011**, *115*, 8131.

27. Taniike, T.; Terano, M.; *J. Catal.* **2012**, *293*, 39.

28. Glaser, R.; Sun, X.; *J. Am. Chem. Soc.* **2011**, *133*, 13323.

29. Yang, W.; Chen, Y.; Sun, W.-H.; *Macromol. Chem. Phys.* **2014**, DOI: 10.1002/macp.201400141

30. Xiao, T.; Zhang, S.; Kehr, G.; Hao, X.; Erker, G.; Sun, W.-H.; *Organometallics* **2011**, *30*, 3658.

31. Delley, B.; *J. Chem. Phys.* **1990**, *92*, 508.

32. Dolg, M.; Wedig, U.; Stoll, H.; Preuss, H.; *J. Chem. Phys.* **1987**, *86*, 866.

33. Bergner, A.; Dolg, M.; Kuechle, W.; Stoll, H.; Preuss, H.; *Mol. Phys.* **1993**, *80*, 1431.

34. Perdew, J. P.; Wang, Y.; *Phys. Rev. B* **1992**, *45*, 13244.

35. Becke, A. D.; *J. Chem. Phys.* **1988**, *88*, 2547.

36. Deng, L.; Margl, P.; Ziegler, T.; *J. Am. Chem. Soc.* **1999**, *121*, 6479.

37. Bryliakov, K. P.; Semikolenova, N. V.; Zudin, V. N.; Zakharov, V. A.; Talsi, E. P.; *Catal. Commun.* **2004**, *5*, 45.

38. Khoroshun, D. V.; Musaev, D. G.; Vreven, T.; Morokuma, K.; *Organometallics* **2001**, *20*, 2007.

39. Scott, J.; Gambarotta, S.; Korobkov, I.; Budzelaar, P. H. M.; *J. Am. Chem. Soc.* **2005**, *127*, 13019.

40. Brookhart, M.; Green, M. L. H.; *J. Organomet. Chem.* **1983**, *250*, 395.

41. Jordan, R. F.; *J. Chem. Educ.* **1988**, *65*, 285.

42. Alelyunas, Y. W.; Jordan, R. F.; Ekhols, S. F.; Borkowsky, S. L.; Bradley, P. K.; *Organometallics* **1991**, *10*, 1406.

43. Jordan, R. F.; Bajgur, C. S.; Willett, R.; Scott, B.; *J. Am. Chem. Soc.* **1986**, *108*, 7410.

44. Fayet, G.; Raybaud, P.; Toulhoat, H.; de Bruin, T.; *J. Mol. Struc-Theochem.* **2009**, *903*, 100.